Poster Session 6: Transplant, Basic Science, Adrenal, Innovation
Sunday, June 30, 2024 • 16:10–17:40

Cite as: *Can Urol Assoc J* 2024;18(6Suppl1):S71-80. http://dx.doi.org/10.5489/cuaj.8831

MP 6.1

Histology of explanted polypropylene vaginal meshes used to treat pelvic floor disorders

Mathilde Rousseau[1], Robert Guidoin[1], Chaojing Li[2], Yile Sun[1], Shiwei Zhao[1], Yuling Wu[1], Caroline Rhéaume[3], Gaétan Le-Bel[1], Eric Philippe[1], Lucie Germain[1], Lu Wang[2], Gaetan Brochu[1], Ze Zhang[1], Genevieve Nadeau[1]

[1]Department of Surgery, Faculty of Medicine, Université Laval and Axe de Médecine Régénératrice, Centre de Recherche du CHU de Québec–Université Laval, Quebec City, Canada; [2]Key Laboratory of Textile Science & Technology, Ministry of Education and College of Textiles, Donghua University, Shanghai, China; [3]Department of Obstetrics and Gynecology, Faculty of Medicine, Université Laval, Centre de Recherche du CHU de Québec–Université Laval, Quebec City, Canada

Introduction: In 2011, medical regulatory authorities issued warnings regarding use of polypropylene transvaginal mesh (TVM) to treat pelvic floor disorders due to rare but severe complications they may cause. Herein, we report a comprehensive histologic examination of explanted TVM to help better understand their biocompatibility and to compare the mechanism of biointegration and/or failure of these devices and their correlation with clinical histories.

Methods: Tissue samples were retrieved from the explants that were afterward worked up using a uniform protocol and then submitted to three analyses: gold-palladium coating for electron microscopy scanning, embedded in paraffin and subjected to various staining solutions for light microscopy, and transmission electron microscopy. Control sampling from identical commercially available devices was analyzed for baseline comparisons.

Results: Seven TVM had been implanted in seven patients (pelvic organ prolapse, n=4; stress urinary incontinence, n=3). Indications for explantation included vaginal mesh exposure (n=5), bladder mesh exposure (n=1), and recurrent prolapse requiring re-do surgery (n=1). The mean interval between implantation and explantation was 38 (4–81) months. The histologic examination of the explants revealed various morphologies, such as fractures in the oxidized surface layer of the polypropylene causing its degradation; dense encapsulations of the polypropylene fibers leading to the formation of scar tissue where bundles of collagen were stretched (rather than undulating) and ruptured as the result of shrinkage; or bacterial colonization associated with a considerable lysis in the collagen ingrowth and large amounts of white blood cells.

Conclusions: Our analysis demonstrated that the lack of biostability illustrated by continuous fragmentations in the oxidized surface is likely to exacerbate a continuous inflammatory reaction. More specifically, mishandling the polypropylene fibers is likely to initiate in vivo degradation and permanently damage the material. Polypropylene then oxidizes on its surface, creating a skin that can be uplifted and fragmented. Flakes of polypropylene are then dispersed in the surrounding tissue, which exacerbates the foreign body tissue reaction. These findings may have significant implications for the implant procedure since such a degradation process may be a contributing factor to eventually developing a mesh-related complication.

MP 6.2

The protective effects of butyrate in kidney stone disease

Sarah Hanstock[1], Demian Ferreira[1], Hans Adomat[1], Felipe Eltit[1], Breanna Nelson[1], Dalia Othman[1], Qiong Wang[2], Anne Haegert[1], Yen-Yi Lin[1], Stephane Le Bihan[1], Roman Herout[1], Rizhi Wang[2], Aaron Miller[3], Genelle Lunken[4], Ben H. Chew[1], Dirk Lange[1]

[1]Department of Urologic Sciences, University of British Columbia, Vancouver, Canada; [2]Department of Materials Engineering, University of British Columbia, Vancouver, Canada; [3]Department of Cardiovascular and Metabolic Sciences, Lerner Research Institute, Cleveland Clinic, Cleveland, United States; [4]Department of Pediatrics, University of British Columbia, Vancouver, Canada

Introduction: Microbiome dysbiosis is suggested as a risk factor for kidney stone disease (KSD). Specifically, individuals with KSD have a lower abundance of intestinal butyrate-producing bacteria. Our study aimed to examine the role of butyrate in calcium oxalate (CaOx) kidney stone formation.

Methods: We developed a novel sodium oxalate diet-induced murine model of hyperoxaluria to assess the effect of supplementing inulin (prebiotic) and tributyrin (butyrate prodrug). Urine and stool samples were collected for oxalate measurements using high performance liquid chromatography/mass spectrometry (HPLC/MS). Stool samples and cecal contents were collected for 16S sequencing and butyrate analysis. Renal tissue was collected for histology to quantify crystal deposits, and for mRNA sequencing (mRNA-seq) to investigate gene expression.

Results: Supplementation of tributyrin in animals fed a high oxalate diet resulted in a significant decrease in renal CaOx crystal deposits versus animals on the oxalate diet alone ($p<0.001$). Inulin supplementation did not attenuate crystal formation. SCFA analysis revealed that inulin supplementation was able to significantly increase butyrate concentration in the stool ($p<0.001$), however, in combination with oxalate this increase was not seen. Microbiome analysis demonstrates that oxalate is a disruptor of the microbiome, and particularly interferes with microbes associated with butyrate production. HPLC/MS analysis revealed that neither urine nor stool oxalate levels were affected by either inulin or tributyrin supplementation. Preliminary mRNA-seq results indicate that tributyrin may have its anti-lithogenic effects because of modifications of pathways related to oxidative stress.

Conclusions: Tributyrin appears to attenuate crystal formation in mice that are on a high oxalate diet and may do this by modulating oxidative stress pathways. Findings from this study may provide insight into the etiology of KSD, and inform the development of novel diet-based strategies to prevent KSD.

MP 6.3

Using unsupervised clustering to characterize novel phenotypes among older kidney transplant recipients: A cohort study

Sareen Singh[1], Syed Sibte Raza Abidi[2], Syed Asil Ali Naqvi[2], Amanda J. Vinson[3], Thomas A.A. Skinner[4], George Worthen[3], Samina Abidi[2,5], Kenneth A. West[3], Karthik K. Tennankore[3]

[1]Faculty of Medicine, Dalhousie University, Halifax, Canada; [2]Faculty of Computer Science, Dalhousie University, Halifax, Canada; [3]Division of Nephrology, Department of Medicine, Dalhousie University, Halifax, Canada; [4]Department of Urology, Queen's University, Kingston, Canada; [5]Department of Community Health and Epidemiology, Dalhousie University, Halifax, Canada

Introduction: Older kidney transplant recipients are at a higher risk of graft failure compared to younger recipients. Existing risk-stratification tools may inadequately capture the diverse recipient factors that could negatively impact post-transplant outcomes in older adults. We applied an unsupervised machine learning-based clustering approach to characterize older kidney transplant recipients. Post-transplant outcomes were assessed for each cluster and for different donor-recipient pairings.

Methods: Kidney transplant recipients aged ≥65 years were identified from the Scientific Registry of Transplant Recipients (2000–2017). We used unsupervised

MP 6.3. Table 1. Post-transplant outcomes according to recipient cluster

Outcome	Cluster 1 (n=6153)	Cluster 2 (n=4813)	Cluster 3 (n=5398)
Primary outcome			
All-cause graft failure			
%	51.7	56.0	58.7
HR (95% CI)	0.93 (0.89-0.98)	1 [Reference]	1.26 (1.20–1.33)
Adjusted HR (95% CI)[a]	0.95 (0.90-1.00)	1 [Reference]	1.25 (1.19–1.32)
Secondary outcomes			
Death despite kidney function			
%	38.4	42.3	44.5
HR (95% CI)	0.92 (0.87-0.97)	1 [Reference]	1.30 (1.22–1.37)
Adjusted HR (95% CI)[a]	0.92 (0.87-0.98)	1 [Reference]	1.29 (1.21–1.37)
Death censored graft failure			
%	13.3	13.7	14.2
HR (95% CI)	0.98 (0.88-1.08)	1 [Reference]	1.17 (1.05–1.29)
Adjusted HR (95% CI)[a]	1.02 (0.92-1.13)	1 [Reference]	1.14 (1.03–1.27)
Delayed graft function			
%	22.7	24.1	31.6
OR (95% CI)	0.93 (0.85-1.01)	1 [Reference]	1.45 (1.33–1.59)
Adjusted OR (95% CI)[a]	0.96 (0.87-1.05)	1 [Reference]	1.42 (1.29–1.55)

[a]Adjusted for donor factors (age, sex, race, height, weight, body mass index category, cytomegalovirus status, diabetes, hypertension, hepatitis C virus, cerebrovascular cause of death, donation after cardiac death, vasodilator use, arginine use, inotrope use, serum creatinine level), cold ischemia time, and number of human leukocyte antigen mismatches.

MP 6.3 Table 2. Time to all-cause graft failure according to different Kidney Donor Risk Index and recipient cluster pairings

	Hazard ratio (95% CI)[a]	
	KDRI <1.45	KDRI ≥1.45
Cluster 1	0.94 (0.88–1.01)	1.36 (1.26–1.46)
Cluster 2	1 [Reference]	1.42 (1.32–1.54)
Cluster 3	1.29 (1.20–1.39)	1.73 (1.61–1.86)

[a]Adjusted for donor sex, donor body mass index, donor cytomegalovirus status, donor vasodilator use, donor arginine use, donor inotrope use, cold ischemia time, and number of human leukocyte antigen mismatches.

clustering to generate phenotypes using 16 recipient factors. We paired the recipient clusters with subgroups of the Kidney Donor Risk Index (KDRI) to create a spectrum of donor-recipient risk profiles. The primary outcome of all-cause graft failure was analyzed using multivariable Cox regression.

Results: Overall, 16 364 patients (mean age 69.4 years; 38% female) were separated into three distinct clusters. Cluster 1 recipients were more likely to be female, cluster 2 recipients were more likely to be white males without diabetes, and cluster 3 recipients were more likely to be males with comorbidities and a longer pre-transplant dialysis vintage. Compared to cluster 2, the risk of all-cause graft failure was lower in cluster 1 (adjusted hazard ratio [aHR] 0.95, 95% CI 0.90–1.00) and higher in cluster 3 (aHR 1.25, 95% CI 1.19–1.32) (Table 1). All recipient clusters had a higher risk of all-cause graft failure when receiving kidneys from donors with a KDRI ≥1.45 (Table 2).

Conclusions: In a nationally representative cohort of older kidney transplant recipients, unsupervised clustering generated clinically distinct recipient phenotypes at differential risks of graft failure. These phenotypes may aid in complementing allocation decisions and optimizing post-transplant care for older recipients.

Acknowledgements: Sareen Singh received a Dalhousie Faculty of Medicine Dr. Tom Marrie Research in Medicine Summer Studentship to support this work.

MP 6.4

Virtual reality in pain management during extracorporeal lithotripsy sessions: A randomized pilot study

Roxann Thériault[1], Carmen-Édith Belleï-Rodriguez[2,3], Marie-Philippe Harvey[2,3], Aurélie Flaive[2,3], Serge Marchand[2], Guillaume Léonard[2,3], Samuel Lagabrielle[1]

[1]Department of Urology, Sherbrooke University Hospital Center, Sherbrooke, Canada; [2]Aging Research Center, Sherbrooke University Hospital Center, Sherbrooke, Canada; [3]Faculty of Medicine and Health Sciences, Sherbrooke University, Sherbrooke, Canada

Introduction: Extracorporeal shockwave lithotripsy (ESWL) is an effective but painful treatment modality for kidney stone disease, which may require the use of opioids. Virtual reality (VR) creates an immersive environment that could reduce the perception of pain. The objective of this randomized pilot clinical trial was to evaluate the feasibility of the protocol and the effect of VR on pain and opioid consumption.

Methods: Patients with radiopaque kidney stones undergoing ESWL for the first time were randomized 2:1 into VR or control group, targeting a sample size of 30 participants. The VR group wore headsets producing a visual and audio stimulation for 20 minutes before ESWL, while the control group had a break in a quiet room. Pain intensity was assessed using a visual analog scale. Fentanyl consumption was recorded by a dose of 50 mcg injected upon patient request. Technicians performing the ESWL sessions were blinded to group allocation and followed the same protocol to gradually increase the intensity of the ESWL.

Results: Out of 188 ESWL done in our institution from November 2022 to December 2023, 68 patients were eligible. As of today, 18 were included (10 in VR group, eight in control group; mean age 58, range 21–82). VR was well-tolerated, except for one patient who asked to stop after five minutes. Although not statistically significant, preliminary results indicate that VR patients tolerated a higher ESWL power (92.5% vs. 84.4%, p=0.24), and fentanyl consumption was also lower in the VR group (0.9 doses) compared to controls (1.5 doses, p=0.29). Pain intensity was lower in the VR group (3.3/10) compared to controls (6.1/10, p<0.05).

Conclusions: Preliminary results show promising outcomes of VR during ESWL in terms of pain reduction and fentanyl use, while being well-tolerated by patients. The implementation of an adequately powered randomized controlled trial will face a low recruitment rate and appropriate strategies will have to be elaborated.

Acknowledgements: Financed by Lucine Enterprise and Dr. Lagabrielle's personal research fund

MP 6.5

Safety and efficacy of prostate embolization using only mobile C-arm in an office-based laboratory setting: A pilot study

Kan Zhang[1], Ralph Madeb[2], Shlokah Hira[3], Arya Bisen[4], Felix Tse[5], Hwunjae Lee[6]

[1]Interventional Radiology, Carepoint Healthcare, Jersey City, United States; [2]Department of Urology, Maimonides Medical Center, New York, United States; [3]School of Medicine, Cardiff University, Watford, United Kingdom; [4]School of Medicine, Bharati Vidyapeeth Medical College, Pune, India; [5]Early Interventional Institute, New York, United States; [6] Department of Radiology, Yonsei University, Yonsei, Korea

Introduction: This is the first known study to measure the feasibility, safety, and clinical outcome of prostate embolization to treat benign prostate hyperplasia with hematuria in an office-cased laboratory (OBL) setting using only mobile C-arm.

Methods: Thirty-six patients underwent percutaneous prostate embolization from November 2020 to June 2021, all with hematuria. All patients have been on long-term therapy with either 5α-reductase inhibitors and/or 1-adrenoreceptor antagonists. The mean age was 64 (range 53–87) years, mean prostate volume was 99 (range 43–262) mL, and three patients had complete obstruction requiring Foley catheter prior to procedure, all from 2020. Thirty-three patients

did not have Foley catheter during the procedure. All procedures used mobile C-arm without rotational CT capabilities (Philips Veridius). Zero patients had CTA of the prostatic artery prior to embolization. Two patients had only left prostatic artery embolization due to vessel tortuosity. Right groin CFA access, RBT catheters (Cooke), and Progreat coaxial microcatheter system (Terumo) were used in all cases. Three patients required additional Renegade catheter and Transcend wires (Boston Scientific). PVA particles (Cooke) were used to embolize until stasis in the prostatic arteries. All patients underwent urology consult ruling out other etiology of LUTS.

Results: The mean contrast volume was 133 (range 80–200). The mean dose was 164.1 (range 76.3–224.4) Gy · cm2, with a mean total procedure time of 49 (range 33–210) minutes. The mean pre-procedure IPSS score was 28.4 and the mean post-procedure IPSS was 14.1, with a mean followup time of five months. No patients had hematuria post-treatment. Three patients had symptoms of urinary urgency post-procedure and had pre-embolization prostate volumes of 132, 150, and 186. There were no other major complications.

Conclusions: Prostate embolization is feasible, safe, and effective in treating BPH in an OBL setting using only a mobile C-arm without the need for Foley catheter insertion.

References:

1. Teichgräber U, Aschenbach R, Diamantis I, et al. Prostate artery embolization: Indication, technique, and clinical results. *Rofo* 2018;190:847-55. https://doi.org/10.1055/a-0612-8067
2. Young S, Golzarian J. Prostate artery embolization: State of the evidence and societal guidelines. *Tech Vasc Interv Radiol* 2020;23:100695. https://doi.org/10.1016/j.tvir.2020.100695
3. Sabharwal T, Popert R. Prostate artery embolization. *BJU Int* 2018;122:167-8. https://doi.org/10.1111/bju.14409
4. Knight GM, Talwar A, Salem R, et al. Systematic review and meta-analysis comparing prostatic artery embolization to gold-standard transurethral resection of the prostate for benign prostatic hyperplasia. *Cardiovasc Intervent Radiol* 2021;44:183-93. https://doi.org/10.1007/s00270-020-02657-5
5. Ray AF, Powell J, Speakman MJ, et al. Efficacy and safety of prostate artery embolization for benign prostatic hyperplasia: An observational study and propensity-matched comparison with transurethral resection of the prostate (the UK-ROPE study). *BJU Int* 2018;122:270-82. https://doi.org/10.1111/bju.14249
6. Insausti I, Sáez de Ocáriz A, Galbete A, et al. Randomized comparison of prostatic artery embolization vs. transurethral resection of the prostate for treatment of benign prostatic hyperplasia. *J Vasc Interv Radiol* 2020;31:882-90. https://doi.org/10.1016/j.jvir.2019.12.810

MP 6.5. Table 1. Feasibility and efficacy ay a glance

Variables	Mean	SD
Contrast volume	133.2 cc	13
Procedure time	49minutes	17.1
Radiation dose	164.1 Gy · cm2	28.3
Foley needed for procedure	0	NA
Pre embolization IPSS	28.4	4.8
Post embolization IPSS	14.1	3.3
Major complication	0	NA
Decrease in IIEF (International Index of Erectile Function)	0	NA

MP 6.6

Subureteric injection for the treatment of vesicoureteral reflux in transplant kidneys

M.Irfan Donmez[1], M.Firat Ozervarli[1], Erdem Ozatman[1], Ismail Selvi[1], Tayfun Oktar[1], Orhan Ziylan[1], Tzevat Tefik[1], Oner Sanli[1], Taner Kocak[1], Aydin Turkmen[2], A. Serra Artan[2], Ismet Nane[1]

[1]Department of Urology, Istanbul University Istanbul Faculty of Medicine, Istanbul, Turkey; [2]Department of Nephrology, Istanbul University Istanbul Faculty of Medicine, Istanbul, Turkey

Introduction: Treatment of de novo vesicoureteral reflux (VUR) into the transplanted kidney constitutes a clinical challenge. The aim of this study was to present our data on patients who underwent endoscopic subureteric injection for the treatment of VUR following renal transplantation (RT) in our center.

Methods: The patients who underwent endoscopic subureteric injection for VUR into the transplanted kidney after RT in our department between 2008 and 2023 were reviewed retrospectively. Indication for subureteric injection, age, gender, laterality, number of injections, amount of material used, renal failure etiology, auxiliary procedures, and treatment success were noted. All interventions were performed by pediatric urologists who also perform RT.

Results: During a median followup of 27.5 (4–160) months, 22 patients (17 women, 77.2%) and 23 transplanted ureters (13 right, eight left, one bilateral) were treated with subureteric injections. In all patients, the indications for subureteric injection were recurrent febrile UTI and the grades of VUR varied from I–IV. Patients received a median of 1.65 cc (0.7–2.7) dextranomer-hyaluronic acid copolymer. In total, 10 RT (eight from living donors, two from cadaveric donors) were performed in another center, whereas 13 RT were carried out in our center (eight from cadaveric donors and five from living donors). Among the patients who were transplanted in our center, the rate of subureteric injections due to de novo symptomatic VUR after RT was 2.2% (13 of 593 patients). After subureteric injections, five patients required a second injection due to the recurrence of VUR. Ureteroureterostomy (to the native ureter) was performed in two patients who had further UTIs after the second endoscopic treatment. Eventually, 19 of 21 patients (90.4%) benefited clinically from the endoscopic treatment and none of the patients underwent re-do ureteroneocystostomy. It is noteworthy that the etiology of renal failure was VUR nephropathy in seven (31.8%) patients.

Conclusions: Subureteric injection provides a high clinical success for the treatment of de novo VUR after RT.

MP 6.7

Controlled rewarming of kidneys from donors after cardiac death is associated with improved early graft function in transplant kidney recipients

Jirong Lu[1,2], Edem Afenu[1], Martin Igbokwe[1], Atheer Alqahtani[1], Ram Patel[3], Yanbo Guo[1,4], Juliano Offemi[1,5], Alp Sener[1], Patrick P. Luke[1]

[1]Department of Surgery, Western University, London Ontario, Canada; [2]Department of Surgery, National University Hospital, Singapore, Singapore; [3]Schulich School of Medicine and Dentistry, Western University, London Ontario, Canada; [4]Department of Surgery, McMaster University, Ontario, Canada; [5]Department of Surgery, University of Manitoba, Manitoba, Canada

Introduction: We and others have shown that donor kidneys warm up to 15°C approximately 10 minutes upon removal from hypothermic storage during vascular anastomosis in kidney transplantation. We hypothesize that rewarming kidneys over 10 minutes (controlled rewarming) is superior to immediate rewarming or uncontrolled rewarming (allowing the kidney to rewarm during the anastomosis).

Methods: From 2018–2023, we reviewed early graft outcomes of DCD kidney transplants. In a limited number of cases, an 'ice blanket' was created using a laparotomy sponge lined with freshly crushed ice and wrapped around the graft during the vascular anastomosis. Recipients were divided into three groups: controlled rewarming (removal of the ice 10 minutes prior to vascular unclamping), immediate rewarming (removal at the time of unclamping), and no ice blanket use (uncontrolled rewarming). Early graft outcomes were analyzed and compared between the three groups using 3x2 Chi-squared and Kruskal Wallis tests. A logistic regression was carried out to assess the effects of ice blanket use, donor and recipient parameters on delayed graft function (DGF).

Results: Of 145 cases, the ice blanket was not used in 86 (59.3%) recipients. Immediate rewarming occurred in 40 (27.6%) and controlled rewarming occurred in 19 (13.1%) patients at a median time of 11 minutes (IQR 10–12).

MP 6.6. Table 1. Clinical course and data of the patients

Patient no	VCUG grade before injection therapy	eGFR before injection therapy (ml/min/1.73m²)	Age at injection therapy (year)	Period from transplantation to injection (months)	Total amount of Dx/HA injection (ml)	Febrile UTI after injection therapy	2nd procedure	Period from the last procedure to timing of final followup (months)	eGFR at the final followup examination
1	4	34	30	120	1.6	-	-	15	N/A
2	4	23	37	84	0.7	-		12	11
3	4	8	18	132	1.4	-		31	12
4	3	58	31	15	1.2	-		8	57
5	2	28.2	36	192	1.7	+	2nd Dx/HA injection 1.5 ml (3 years after 1st injection	18	26.6
6	4	N/A	14	15	2	-	-	61	11
7	3	75	50	102	2.4	-	-	26	74
8	3	N/A	11	84	0.9	-	-	160	5
9	3	27.9	46	35	1	+	2nd Dx/HA injection 1.5 ml (21 months after 1st injection)	49	13.4
10	4	132	53	180	1	+	2nd Dx/HA injection 0.7 ml (3 months after 1st injection)	29	51.5
11	4	92	44	4	1.5	-		94	52.9
12	3	N/A	50	132	1.7	-		142	47
13	4	N/A	44	216	2	-		5	N/A
14	3	N/A	50	111	2.7	-		63	24.5
15	3	N/A	29	16	1.7	-		8	N/A
16	3	85	36	44	1.7	-		75	82.4
17	1	N/A	41	60	2	-		132	40.75
18	3	48	52	204	2	-		60	36
19	3	82	40	132	1.5	+	2nd Dx/HA injection 1.5 ml (4 months after 1st injection)	6	80
20	4	74	35	168	1.3	-		12	79.8
21	3	51	52	61	0.9	+	2nd Dx/HA injection 0.7 ml (5 months after 1st injection) Ureteropyelostomy 4 months after 2nd injection)	4	50.5
22	4	45	20	4	2.4	+	2nd Dx/HA l injection 2.5 ml (3 months after 1st injection) Ureteroureterostomy 5 months after 2nd injection)	8	58

Donor, recipient and transplant parameters were similar between groups. DGF rates were 65% (immediate rewarming) vs. 45% (uncontrolled) vs. 16% (controlled rewarming) (p=0.002), with all pairwise comparisons being statistically significant. eGFR was highest in the controlled rewarming group at one month (p=0.026), but not sustained at three months between groups (p=0.347). On multivariable logistic regression, donor age, recipient years on dialysis, and ice blanket use were significant. Compared to uncontrolled rewarming, DGF rates were more likely with immediate rewarming (OR 2.86, 95% CI 1.12–7.27, p=0.028) and less likely with controlled rewarming (OR 0.14, 95% CI 0.03–0.62, p=0.010). **Conclusions:** Controlled 10-minute rewarming of donor kidneys is associated with superior early graft function compared with uncontrolled rewarming and immediate rewarming of kidneys. Continued analysis of greater numbers and randomized controlled trials are required to validate these findings.

MP 6.7. Table 1. Donor, recipient, and transplant parameters

	Uncontrolled rewarming, n=86	Immediate rewarming, n=40	Controlled rewarming, n=19	p
Donor parameters				
Age	43.2 (34.7–57.2)	43.4 (33.7–53.6)	42.6 (30.5–51.2)	0.5778
Sex (male)	51 (59.3)	33 (82.5)	8 (42.1)	0.00414
BMI	26 (23.6–31.6)	26.6 (23.6–29.6)	29.1 (23.1–33.4)	0.6163
Recipient parameters				
Age (y)	56.3 (47–64.3)	56.2 (45.7–64.3)	56.3 (38–62)	0.8344
Sex (male)	54 (62.8)	22 (55)	13 (68.4)	0.5708
BMI	28.2 (24.8–31.8)	26.8 (23.6–32.2)	27.41 (25.2–31.1)	0.8589
Dialysis vintage (y)	2.3 (1.4–2.9)	2.3 (1.7–2.9)	2.4 (1.4–3.8)	0.8147
Transplant parameters				
Warm ischemia time (min)	32 (27–67)	30 (24–45)	33 (27–82)	0.3349
Cold ischemia time (h)	8.9 (6.4–11.7)	8.9 (6.3–11.8)	8.9 (6.1–12.3)	0.9201
Anastomotic time (min)	39 (32–46)	41 (34.5–44.5)	37 (32.5–42.5)	0.454

Values are median (IQR) or n (%).

MP 6.7. Table 2. Early graft outcomes between rewarming groups

	Uncontrolled rewarming, n=86	Immediate rewarming, n=40	Controlled rewarming, n=19	p
DGF	39 (45.3)	26 (65)	3 (15.8)	0.002
Serum creatinine (μmol/L)				
7 days	469 (208–671)	531 (262–656)	280 (178–516)	0.148
1 month	140 (107–211)	119 (98–155)	113 (93–143)	0.036
3 months	125 (101–183)	121 (90–141)	115 (103–150)	0.490
eGFR (ml/min/1.73m^2)				
7 days	10.0 (7.6–27.4)	8.5 (6.9–20.3)	19.4 (9.8–38.5)	0.111
1 month	46.2 (28.8–62.6)	56.8 (43.1–69.2)	60.9 (44.1–78.3)	0.026
3 months	52.9 (33.9–70.3)	56.1 (43.2–84.9)	60.3 (49.5–76.7)	0.347

Values are median (IQR) or n (%).

MP 6.8

A novel, non-destructive stone analysis technique with micro-X-ray fluorescence and electron microprobe

Mario Basulto-Martínez[1], Lauren Stone[2], Tariq Alotaibi[1], Jeremy Burton[3], Hassan Razvi[1], Jennifer Bjazevic[1]

[1]Division of Urology, Western University, Schulich School of Medicine & Dentistry, London, Canada; [2]Earth and Planetary Materials Analysis Laboratory, Western University, London, Canada; [3]Department of Microbiology & Immunology, Western University, London, Canada

Introduction: Urinary stone composition should be investigated whenever feasible to target prevention strategies and decreased stone recurrence rates; however, modern techniques for urinary stone analysis are typically limited to mass spectrometry, spectroscopy, and powder X-ray diffraction. Although efficient, these techniques require pulverization prior to analysis, preventing investigation of the internal heterogeneity exhibited by some stones. Therefore, we aimed to use non-destructive methods of spectrochemical analysis to determine the spatial distribution of elements within the stones at the micron scale and gain a greater understanding of the underlying mechanisms of stone formation.

Methods: Five human kidney stones were embedded in resin, cross-sectioned, and polished prior to geochemical analyses via two techniques: micro-X-ray fluorescence (μXRF) and electron microprobe analysis (EPMA). Both techniques used highly restricted excitation beams to determine the elemental composition of micron-scale "spots." Overlapping spots were scanned until the full sample surface had been covered, allowing for the generation of high-

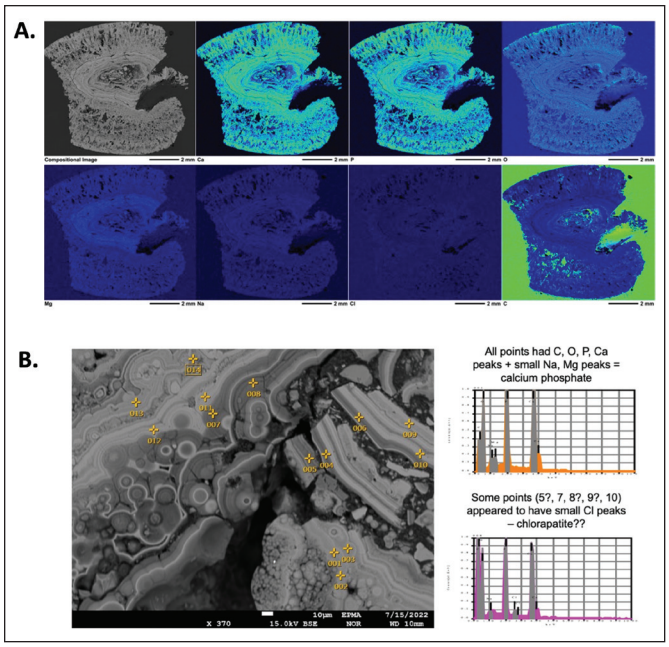

MP 6.8. Figure 1.

resolution maps of elemental/mineralogical distribution within the stones. μXRF was conducted with the Bruker M4 Tornado and the JEOL JXA-8530F microprobe instrument for EPMA. All analyses were carried out at the Earth and Planetary Materials Analysis.

Results: Five stones were analyzed with the following compositions: 1) calcium phosphate (CaPO); 2) calcium oxalate (CaOx) with a cysteine band; 3) uric acid (UA) with CaOx bands; 4) CaOx with CaPO at the surface; and 5) UA with CaPO and CaOx bands. Moreover, spatially resolved elemental identification was achieved, allowing for compositional mapping of the major types of stones and locations of trace elements (e.g., Na, Zn, Cu) (Figure 1).

Conclusions: This proof-of-concept study demonstrates the feasibility of using non-destructive techniques for human urinary stone composition analysis using μXRF and EPMA, and allowed us to identify unique trace elements present within all five stones Further studies matching stone composition and patients' clinical data are warranted to better understand the underlying mechanisms of stone crystallization and how trace elements may impact this process.

MP 6.9

Weighing the options: Surgical and medical management of unilateral aldosterone excess demonstrate distinct profiles of benefits and harms

Maria Salman[1,2], Anique Le Roux[3], Gregory Hundemer[1,2], Neal Rowe[1,3]
[1]Department of Medicine, University of Ottawa, Ottawa, Canada; [2]Department of Nephrology, The Ottawa Hospital, Ottawa, Canada; [3]Department of Urology, The Ottawa Hospital, Ottawa, Canada

Introduction: Primary aldosteronism (PA) is characterized by autonomous aldosterone production that may lead to hypertension and hypokalemia in affected patients. One-third of such patients have unilateral disease, which was our study's focus. The main treatment options for unilateral disease include adrenalectomy or mineralocorticoid receptor antagonists (MRA), with each treatment carrying its respective risks and benefits. Our study aimed to clarify the benefits and harms of the main treatment modalities to inform patients making treatment decisions.

Methods: We performed a scoping review of the English literature. Medline and Cochrane databases were used to extract meta-analysis, treatment guidelines, and systematic reviews. Inclusion criteria were hyperaldosteronism, drug therapy, prevention and control, surgery, therapy, peer-reviewed, systematic reviews, meta-analyses, and guidelines; exclusion criteria were animal studies, case reports, letters, editorials, and duplicates.

Results: Our search criteria identified 161 studies. Of these, 101 were excluded based on irrelevance, leaving 60 studies that were informative for surgical and medical treatment outcomes. We performed a qualitative analysis. Patients receiving either adrenalectomy or MRA had improved post-treatment blood pressure; however, patients who underwent adrenalectomy were more often on less antihypertensive agents compared to patients on a MRA ($p<0.00001$),[1] and the odds of cardiac events after surgery, including coronary artery disease (OR 0.3, p=0.008), major adverse cardiac events (OR 0.55, p=0.0001), and congestive heart failure (OR 0.52, p=0.004), were reduced.[2] Major complications (1.3%) from surgery included blood loss requiring transfusion, surgical site infections, conversion to open surgery, and mortality.[3] Side effects of MRA therapy include gynecomastia (10%),[4] erectile dysfunction (5.8%),[5] and hyperkalemia (11.2%).[6]

Conclusions: Unilateral aldosterone excess can be managed with either extirpative surgery or a mineralocorticoid antagonist; however, each treatment modality has a unique profile of benefits and risks. These data may facilitate treatment discussions and support shared decision-making.

Acknowledgements: The authors would like to acknowledge Nigèle Langlois, librarian, for her guidance in the literature search.

References:

1. Satoh M, Maruhashi T, Yoshida Y, et al. Systematic review of the clinical outcomes of mineralocorticoid receptor antagonist treatment vs. adrenalectomy in patients with primary aldosteronism. *Hypertens Res* 2019;42:817-24. https://doi.org/10.1038/s41440-019-0244-4
2. Chen SY, Chen JY, Huang WC, et al. Cardiovascular outcomes and all-cause mortality in primary aldosteronism after adrenalectomy or mineralocorticoid receptor antagonist treatment: A meta-analysis. *Eur J Endocrinol* 2022;187:S47-58. https://doi.org/10.1530/EJE-22-037
3. Walz MK, Alesina PF, Wenger FA, et al. Posterior retroperitoneoscopic adrenalectomy--results of 560 procedures in 520 patients. *Surgery* 2006;140:943-8; discussion 948-50. https://doi.org/10.1016/j.surg.2006.07.039
4. Haynes BA, Mookadam F. Male gynecomastia. *Mayo Clin Proc* 2009;84:672. https://doi.org/10.4065/84.8.672
5. Bloch MJ, Basile JN. Spironolactone is more effective than eplerenone at lowering blood pressure in patients with primary aldosteronism. *J Clin Hypertens* 2011;13:629-31
6. Surabenjawong U, Thunpiphat N, Chatsiricharoenkul S, et al. Prevalence of hyperkalemia in adult patients taking spironolactone and angiotensin converting enzyme inhibitors or angiotensin receptor blockers. *J Med Assoc Thai* 2013;96:905-10.

MP 6.10

Mathematical model to assist complex prostate artery selection in complex prostate embolization

Kan Zhang[1], Ralph Madeb[2], Shlokah Hira[3], Arya Bisen[4], Felix Tse[5], Hwunjae Lee[6]
[1]Interventional Radiology, Carepoint Health, Jersey City, United States; [2]Department of Urology, Maimonides Medical Center, New York, United States; [3]School of Medicine, Cardiff Univerity, Watford, United Kingdom; [4]School of Medicine, Bharati Vidyapeeth Medical College, Pune, India; [5]Early Interventional Institute, New York, United States; [6]Department of Radiology, Yonsei University, Yonsei, Korea

Introduction: We aimed to apply a mathematical model to decrease procedure time and increase the success of selecting complex prostatic artery takeoff in prostate embolization for BPH.

Methods: Forty-two patients underwent prostate embolization for BPH and/or hematuria. Twenty-three patients had complex prostatic artery takeoff, defined by a longer than 10-minute attempt for the operator to select the prostatic artery using coaxial microcatheter and wire (2.0 Progreat, Terumo). Therefore, Poisson distribution is used in the model to apply probability mass function based on the ratio between prostatic artery diameter and the higher order arterial branch diameter, using the equation f(k; lambda)= Pr(X=k)= lambda^k* e^(-lambda)/k!, where k is the number of occurrences, lambda = E (X)=Var (X). Lambd=r*t, where t is the time interval needed to select prostatic artery (software used: Microsoft Excel). The wire used is shaped with diameter=2*diameter of higher order arterial branch. Wire torque angles (total 8) were used at 90, 180, 270, 360, -360, -270, -180, and -90 degrees.

Results: All 23 patients had successful selection of prostatic artery. Average real vessel selection time was 17 (range 3–25) minutes. The average modeled

vessel selection time was 9 (range 1–18) minutes, with correlation to real-time 0.77 (p=0.034). Each torque angel used five attempts and once all eight angles were used, the same angles were repeated in the same order until the prostatic artery was selected.

Conclusions: There is a high correlation between time from mathematical model and real time, which increased the probability of success and decreased time in selecting complex prostatic artery anatomy.

References:

1. Ray AF, Powell J, Speakman MJ, et al. Efficacy and safety of prostate artery embolization for benign prostatic hyperplasia: An observational study and propensity-matched comparison with transurethral resection of the prostate (the UK-ROPE study). *BJU Int* 2018;122:270-82. https://doi.org/10.1111/bju.14249
2. Insausti I, Sáez de Ocáriz A, Galbete A, et al. Randomized comparison of prostatic artery embolization vs. transurethral resection of the prostate for treatment of benign prostatic hyperplasia. *J Vasc Interv Radiol* 2020;31:882-90. https://doi.org/10.1016/j.jvir.2019.12.810

MP 6.11

Tuohy-Borst under pressure: Intraoperative limitations quantified

Zizo Al-Daqqaq[1], Egor Parkhomenko[2], Muaiqel Almuaiqel[2], Farah Elnakoury[3], Karim Habib[3], Amir Hamzeh[1], Jonguk Lee[2], Ihtisham Ahmad[1], Brian Carrillo[4], Sufyan Shaikh[2], Monica Farcas[2,5,6]

[1]Temerty Faculty of Medicine, University of Toronto, Toronto, Canada; [2]Division of Urology, St. Michael's Hospital, Toronto, Canada; [3]Faculty of Medicine, Royal College of Surgeons in Ireland, Dublin, Ireland; [4]WellSpring Research, Toronto, Canada; [5]Agnico Eagle Chair in Endourology and Minimally Invasive Surgery, St. Michael's Hospital, Toronto, Canada; [6]Institute for Biomedical Engineering, Keenan Research Centre for Biomedical Science, Toronto, Canada

Introduction: The Tuohy-Borst adapter (T-Ba) is used in ureteroscopy and laser lithotripsy (URSL) to facilitate entry and manipulation of laser fibres and nitinol baskets under pressurized irrigation. Drawbacks of the T-Ba include jet leaks of biohazardous fluids, damaged tools from T-Ba overtightening, and unintended adapter-scope disconnections. This is the first study to quantify these problems in the operating room, with the objective of improving safety while saving healthcare dollars.

Methods: From January to October 2023, 61 URSL cases were observed, with two cases excluded from analysis due to conversion to PCNL, and six diagnostic cases with limited instrumentation. Standard variables were collected, along with number of jet leaks, adapter-scope disconnections, and baskets damaged by the T-Ba. URSL cases were performed by staff endourologists and assisted by junior surgeons ranging from PGY2 to endourology fellow.

Results: Across 53 included cases, there was a mean of 2.26 jet leaks per case and 31 total accidental disconnections. Regarding safety, 13.3% of jet leaks sprayed staff in the face and 10.8% sprayed sterile equipment. There were 0.53 jet leaks per instrument insertion across a sample of 15 cases (Figure 1). Among the 47 cases where a nitinol basket was used, 14 baskets were damaged directly by the T-Ba. The 1.5 Fr baskets were damaged at a rate of 32.5% (13/40), while the 2.4 Fr baskets were damaged at a rate of 11.1% (1/9). The estimated total cost of damaged baskets was approximately $11 000. One-way ANOVA revealed no significant association between the most junior surgeon's level of training and the number of jet leaks (p=0.075), adapter-scope disconnections (p=0.151), or damaged baskets (p=0.37).

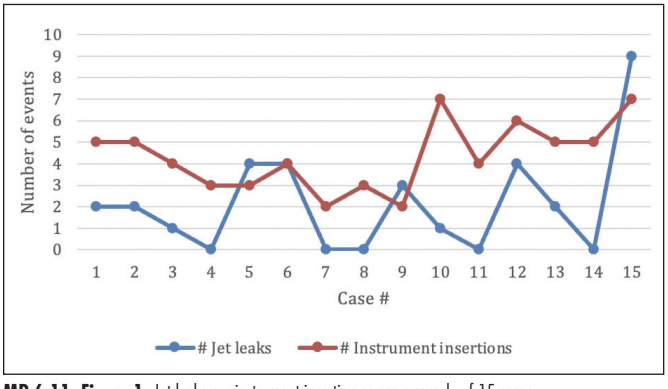

MP 6.11. Figure 1. Jet leaks per instrument insertion across a sample of 15 cases.

Conclusions: The T-Ba has significant drawbacks when used in URSL, which are independent of the surgeon's training level. This study provides strong evidence for the need to develop a novel ureteroscope adapter to address the safety and financial implications of the T-Ba's drawbacks.

MP 6.12

Safety and efficacy of electromotive drug administration in the renal pelvis: First in-vivo porcine study

Bruce M. Gao[1], Seyed Hossein Hosseini Sharifi[1], Michael Wu[1], Zachary E. Tano[1], Seyed Amiryaghoub M. Lavasani[1], Seyedamirvala Saadat[1], Sohrab N. Ali[1], Erika Martinez- Carcamo[1], Mahra Nourbakhsh[2], Pengbo Jiang[1], Roshan M. Patel[1], Michael Daneshvar[1], Jaime Landman[1], Ralph V. Clayman[1]

[1]Department of Urology, University of California Irvine, Orange, United States; [2]Department of Anatomic Pathology, University of California Irvine, Orange, United States

Introduction: Safe and efficient localized drug administration to the renal pelvis is an unmet need given the rapid clearance of any instilled medication secondary to the ongoing flow of urine and its dilutional impact. Previously, we demonstrated that applying electromotive drug administration (EMDA) to the ureter would drive a small positively charged molecule into the ureteral wall. Accordingly, we sought to investigate the safety and efficacy of EMDA in the renal pelvis.

Methods: In a female Yorkshire pig, via an extraperitoneal midline incision, the proximal ureters were sharply transected 2 inches distal to the ureteropelvic junction. An 8 Fr dual lumen catheter and a non- insulated 0.5 mm silver wire jacketed by a 5 Fr catheter fenestrated in three rows (0.3 mm each) in its 5 cm distal end, was inserted into both renal pelvises and secured using a 2-0 silk suture. A dispersive pad was affixed to the ipsilateral flank and connected to the EMDA generator (Physion→ Mini 30N2). Methylene blue (0.1%), a positively charged, water-soluble stain with a molecular weight of 334 Da, was infused via the dual lumen catheter at a rate of 5 ml/min using a drug infusion pump; the other lumen was left open for gravity drainage. A positive pulsed direct current of 4 mA was applied for 20 minutes in the experimental renal pelvis. The same infusion was performed on the contralateral side; however, EMDA was not activated. The pig was euthanized, and both kidneys were excised for histopathological analysis.

Results: As displayed in Figure 1, H&E staining revealed slight denudation of urothelial cells, but no injury to the deeper tissues. Frozen sections of the experimental renal pelvis showed dense, diffuse methylene blue penetration into the urothelium and lamina propria. In contrast, the control kidney exhibited faint methylene blue staining in the urothelium with limited penetration.

Conclusions: EMDA enhanced the penetration of a small, water-soluble charged

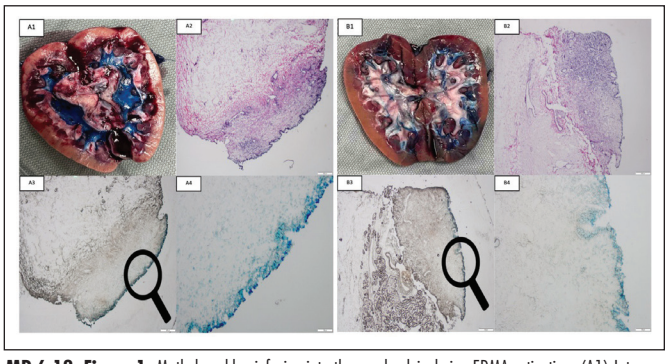

MP 6.12. Figure 1. Methylene blue infusion into the renal pelvis during EDMA activation. (A1) Intense macroscopic staining of the renal pelvis. (A2) H&E staining shows a normal architecture with no signs of acute injury. (A3) (A4) Deep blue staining of the urethral mucosa into the lamina propria of the renal pelvis. Methylene blue infusion into the renal pelvis without EDMA activation. (B1) Faint macroscopic staining of the renal pelvis. (B2) H&E staining shows a normal architecture with no signs of acute injury. (B3) (B4) Minimal staining of the urothelium with scant methylene blue in the lamina propria of the renal pelvis.

molecule into the urothelium and lamina propria of the porcine renal pelvis. Future steps include evaluating EMDA administration of chemotherapeutics such as Mitomycin C in the upper urinary tract.

Acknowledgements: Published in Journal of Endourology October 2023 (Hosseini Sharifi SH, Wu YX, et al Electromotive drug administration (EMDA) in the porcine renal pelvis: First report. J Endourol 2023 Oct 16; Epub ahead of print)

MP 6.13

Temperature changes in the renal allograft warming during kidney transplantation: Comparison of controlled vs. standard rewarming

Martin Igbokwe[1], Jirong Lu[1,2], Atheer Alqahtani[1], Erica Li[3], Alp Sener[1], Patrick P. Luke[1]
[1]Department of Surgery, Western University, London Ontario, Canada; [2]Department of Surgery, National University Hospital, Singapore, Singapore; [3]Schulich School of Medicine and Dentistry, Western University, London Ontario, Canada

Introduction: The effect of temperature changes during re-anastomosis of the kidney into the iliac vessels constitutes a second warm ischemic time (WIT). We have shown that a technique using an ice blanket (IB) wrapped around the kidney, which is removed 10 minutes prior to completion of the anastomosis, can reduce delayed graft function. Some studies have postulated that longer duration of the allograft temperatures >15 degrees Celsius during anastomosis are associated with poorer graft function. This study aimed to identify allograft temperature changes during the second WIT among a cohort of kidney transplant recipients and to compare these temperature changes among kidneys undergoing standard rewarming vs. those undergoing controlled rewarming with the IB technique.

Methods: Using a non-contact DLT model 61–847 infra-red thermometer, the temperature of the kidney was taken at specific time points during the second WIT. Timing was commenced from retrieval of the organ from the perfusion pump/cold storage until the end of anastomosis and re-perfusion. The ambient temperature of the operating room and core body temperature of the recipient were also recorded. Data was analyzed using and expressed as means and standard deviations. A p-value of <0.05 was considered statistically significant. The standard rewarming was compared with the controlled rewarming group.

Results: Twenty-three patients were studied in this preliminary report. There were 14 patients in the standard rewarming group (controls) and nine in the IB group. There were no statistically significant differences in the ambient room and core body temperatures in both study groups. The mean temperatures of the allograft at the time of unclamping and rate of rise were significantly less in the IB group (Table 1) (p= 0.0184 and 0.1336, respectively). The duration the graft temperature measured above 15 degrees Celsius was significantly lower for the IB group (p<0.0001). When compared to standard rewarming, the use of a controlled rewarming contributes to a significantly lower temperature at clamp release, lower overall temperatures at all time points before clamp release (p= 0.0052), and a lower temperature rise per minute (AUC/min) (p<0.0001) (Figures 1, 2).

Conclusions: This preliminary report shows a significant reduction in surface temperature of the renal allograft associated with controlled rewarming techniques. These kidneys also spend a significantly longer duration above 15 degrees Celsius during the second WIT in the standard rewarming group. As preliminary results demonstrate a reduction in delayed graft function and improvement in early graft function in controlled rewarming cases, we continue to assess the long-term outcomes in kidney transplant recipients.

MP 6.13. Table 1. Temperature inferences in standard (no ice blanket) vs. controlled rewarming (ice blanket)

	No ice blanket			Ice blanklet			
	N	Mean	SD	N	Mean	SD	p
Slope of temperature curve before clamp release	14	0.43	0.24	9	0.27	0.24	0.1336
Temperature at clamp release	14	25.21	6.78	9	18.19	5.81	0.0184
Area under curve (AUC) before clamp release	14	589.03	179.29	9	366.78	143.85	0.0052
AUC/min	14	17.22	2.50	9	8.04	4.55	<0.0001
Duration with temperature > 15 degrees C (Minutes	14	23.74	8.46	9	5.39	5.52	<0.0001

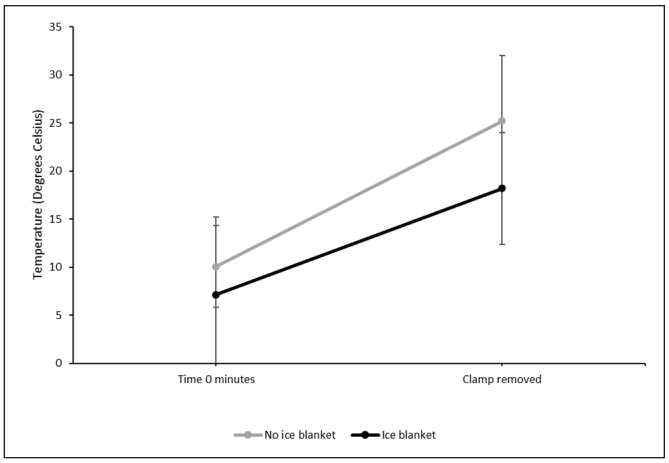

MP 6.13. Figure 2. Mean temperatures in standard (no ice blanket) vs. controlled rewarming (ice blanket).

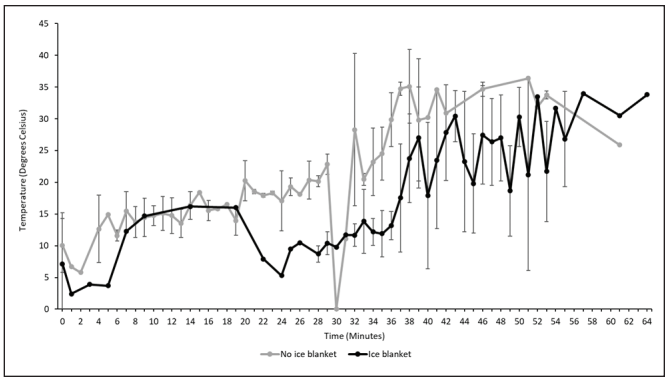

MP 6.13. Figure 1. Temperatures of all kidneys in the standard (no ice blanket) vs. controlled rewarming (ice blanket).

MP 6.14

Perioperative outcomes of adrenal surgery: Does surgical specialty matter?

Basil Ahmad[1], Naji J. Touma[2]
[1]School of Medicine, Queen's University, Kingston, Canada; [2]Department of Urology, Kingston Health Sciences Centre, Kingston, Canada

Introduction: Management of adrenal disease requires a multidisciplinary approach often involving varied specialists, such as endocrinologists, surgeons, oncologists, and medical geneticists. Surgical management has often overlapped between general surgeons usually with an interest in surgical endocrinology, or urologists with minimally invasive surgical skills. The objectives of this study were to assess referral patterns of adrenal cases based on surgical subspecialty, define perioperative outcomes of contemporary adrenal surgery, and whether those outcomes are impacted by the surgeon's subspecialty.

Methods: A retrospective chart review of all adrenalectomies performed at our center from January 2012 to August 2023 was conducted. The only exclusion criterion was when an adrenalectomy was performed secondary to the main procedure, for example, in the case of a radical nephrectomy for renal cell carcinoma. Specific data was collected and grouped under the following categories: patient characteristics, indications for an adrenalectomy, procedural statistics, and perioperative patient outcomes.

Results: A total of 121 adrenalectomies were performed in just over 10 years. Of these, 103 were included in the analysis. Thirty-seven were performed by general surgery, whereas 66 were performed by urology. There were no significant differences in patients' age and Charlson comorbidity score between

the two surgical specialties. The indications for the adrenalectomy were similar between the specialties and were as follows: 32 (31.1%) for pheochromocytoma, 24 (23.3%) for a cortical functional lesion, 19 (18.4%) for a metastasectomy, 16 (15.5%) for size or growth, and 10 (9.7%) for adrenocortical carcinoma. There were no differences in overall operating room time or type of procedure (open/laparoscopic). Most (89.3%) of the procedures were performed laparoscopically. Patients who were operated on by general surgeons were more likely to be readmitted within 30 days than those operated on by urologists (five patients, 13.51% vs. one patient, 1.52%, p=0.04). They were also more likely to require ICU/stepdown ICU admission (19 patients, 51.35% vs. 19 patients, 28.79%, p=0.039). There was no difference in length of stay or postoperative complications. There was, however, one Clavien Dindo 5 complication after a procedure performed by general surgery.

Conclusions: Most adrenalectomies at our center are performed by urology. Indications for adrenalectomy are similar between the specialties. Although postoperative complication rates are similar between the specialties, rates of 30-day readmission and ICU/stepdown admission decreased when urologists performed adrenalectomies. Adrenalectomies may be performed safely by either specialty and factors such as local expertise and surgical volumes are likely more important factors.

MP 6.15

Histologic patterns and recurrence of Hunner lesions in interstitial cystitis/bladder pain syndrome and effectiveness of triamcinolone injection

Hend Alshamsi[1], Claudia Covarrubias[2], Philippe Cammisotto[2], Lysanne Campeau[1,2]
[1]Division of Urology, McGill University, Montreal, Canada; [2]Lady Davis Institute, Jewish General Hospital, McGill University, Montreal, Canada

Introduction: Bladder pain syndrome (BPS)/interstitial cystitis (IC), is a chronic, debilitating condition affecting the bladder and surrounding tissues. It is believed to involve abnormalities in the bladder lining, immune, and nervous system. It can present with Hunner lesions (HL), which feature areas of inflammation and ulceration, causing severe pain and bleeding. Treatment of HL includes fulguration and/or injection of triamcinolone. This study aimed to examine the histopathology and immunostaining of HL and investigate its impact on the severity, progression, recurrence rate, and response to triamcinolone to those who received it.

Methods: We conducted a retrospective chart review of 14 patient demographics (median age of 65.66±16.15 years), clinical characteristics, and treatment outcomes for patients with HL, non-Hunner lesions (NHL), and unaffected controls (UC) who were treated from January 2013 to November 2023. Bladder biopsies were stained with hematoxylin and eosin (H&E) and with antibodies (p75NTR, TNF-alpha, CD68, and E-Cadherin). Data was statistically analyzed using GraphPad Prism 9 software.

Results: This study comprised a total of 14 participants who were monitored for an average duration of six (1–16.9) years. Bladder biopsies were obtained from 13/14 individuals (12 females, one male) with HL IC/BPS (n=6), N-HL IC/BPS (n=3), and UC (n=4). The number and location of HL varied among patients, ranging from one to six lesions, predominantly located at the dome, posterior, and posterolateral walls. All patients with HL underwent various therapies, including medical oral therapy (4/5 patients) and fulguration (4/5 patients). Among the patients with HL, 5/7 (71.4%) received intravesical injection of triamcinolone at the lesion sites, with three patients requiring multiple retreatments due to symptom recurrence up to 3–6 times. One of the seven patients underwent simple cystectomy without a triamcinolone injection trial. Histopathologic analysis revealed acute and chronic inflammatory changes, along with extensive denudation in the HL group, exhibiting more mast cells and fibrosis in the subgroup that received multiple triamcinolone injections. Preliminary results of immunostaining indicated cells positive for TNF-alpha, CD 68, and receptor p75NTR in the lamina propria HL samples, as compared to those with NHL and UC.

Conclusions: Individuals diagnosed with BPS/IC with HL who undergo treatment with triamcinolone have higher recurrence rates, display more pronounced clinical manifestations, pathologic features, and positive immunostaining for TNF-alpha, CD68, and p75NTR when compared to patients with NHL and UC. Further investigations with a larger patient cohort are imperative to validate these observed results.

MP 6.16

Novel insights into a dysregulated calcium handling network in calcium stone formers

John Antonio Chmiel[1,2], Gerrit Alojzi Stuivenberg[1,2], Shannon Seney[1], Kait Al[1,2], Jeremy Paul Burton[1,2,3], Hassan Razvi[3], Jennifer Bjazevic[3]
[1]Centre for Human Microbiome and Probiotic Research, Lawson Health Research, London, Canada; [2]Department of Microbiology and Immunology, Western University, London, Canada; [3]Division of Urology, St. Joseph's Hospital, London, Canada

Introduction: Calcium-based kidney stones constitute approximately 80% of all renal calculi. Despite their prevalence, the underlying pathophysiology is not well understood but is thought to be a result of dysregulated calcium handling by the body. In this study, we investigated the relationship between calcium homeostasis and calcium urolithiasis in a cross-sectional, single-center, adult population.

Methods: Thirty participants with no history of kidney stones and 31 participants who currently or previously (within 12 months) have had at least one a calcium-containing kidney stone were recruited for the study. Participant data, including serum, plasma, spot urine, and medical history, were collected from the participants during the single-study visit.

Results: Preliminary evidence from this study reveals that calcium stone formers exhibit abnormal calcium handling, which is demonstrated by increased blood and urine calcium levels compared to controls. Stone formers also display increased titers of 1,25(OH)2 vitamin D (active form) and reduced urine levels of phosphate, despite similar levels of 25(OH) vitamin D (storage form). Correlation network analysis unveils a calcium-handling network that is unique to stone formers and may begin to explain the differences between stone formers and controls (Figure 1).

Conclusions: This study offers initial evidence to substantiate the impact of impaired calcium regulation, influenced by calcitriol, in stone-related diseases. Nonetheless, additional research is needed to gain deeper insight into changes in calcium handling in stone disease and explore the role of active vitamin D in this process.

Acknowledgements: This work was funded in part by the Northeastern Section of the AUA and a Lawson Health Research Institute Internal Research Fund.

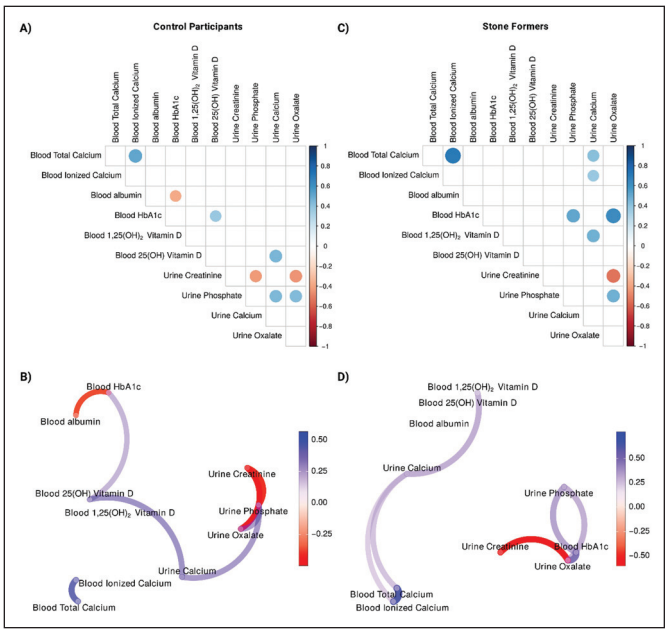

MP 6.16. Figure 1. Correlation matrices of lab results of control and stone former participants. Spearman's rank correlation coefficient matrix from the (A) control and (B) stone former participants. Dots represent significant correlations, with color referring to the correlation coefficient. Network plots of significant relation coefficient from (C) control and (D) stone former participants. Color refers to the correlation coefficient.

MP 6.17

A machine learning model that distinguishes calcium vs. non-calcium stone composition to improve treatment strategies and pathophysiologic insights

John Antonio Chmiel[1,2], Gerrit Alojzi Stuivenberg[1,2], Jennifer Wong[3], Linda Nott[3], Jeremy Paul Burton[1,2,3], Hassan Razvi[3], Jennifer Bjazevic[3]

[1]Department of Microbiology and Immunology, Western University, London, Canada; [2]Centre for Human Microbiome and Probiotic Research, Lawson Health Research, London, Canada; [3]Division of Urology, St. Joseph's Hospital, London, Canada

Introduction: Preventative strategies and surgical treatment for urolithiasis depend on stone composition; however, stone composition is often unknown until the stone is passed or surgically managed. Given that stone composition likely reflects the physiologic parameters during its formation, clinical data from stone formers was used to predict calcium vs. non-calcium stone composition.

Methods: Stone composition, 24-hour collection, serum biochemistry, and biometric data were prospectively collected from calcium (n=625) and non-calcium (n=152) stone patients at a tertiary care center metabolic stone clinic. A training dataset (80% of the data) was used to train a binary gradient-boosted tree (Figure 1A). Class imbalance was addressed by upsampling the minority class and hyperparameters were tuned using Bayesian optimization. A testing dataset (20% of the data) was used to evaluate the model.

Results: The model showed acceptable performance, with an area under the receiver operator characteristics (AUC-ROC) curve of 0.76 (Figure 1B). Sensitivity and specificity were 0.86 and 0.73, respectively (Figure 1C). 24-hour urine calcium, blood urate, and blood phosphate were the most important predictors for the classification (Figure 1D).

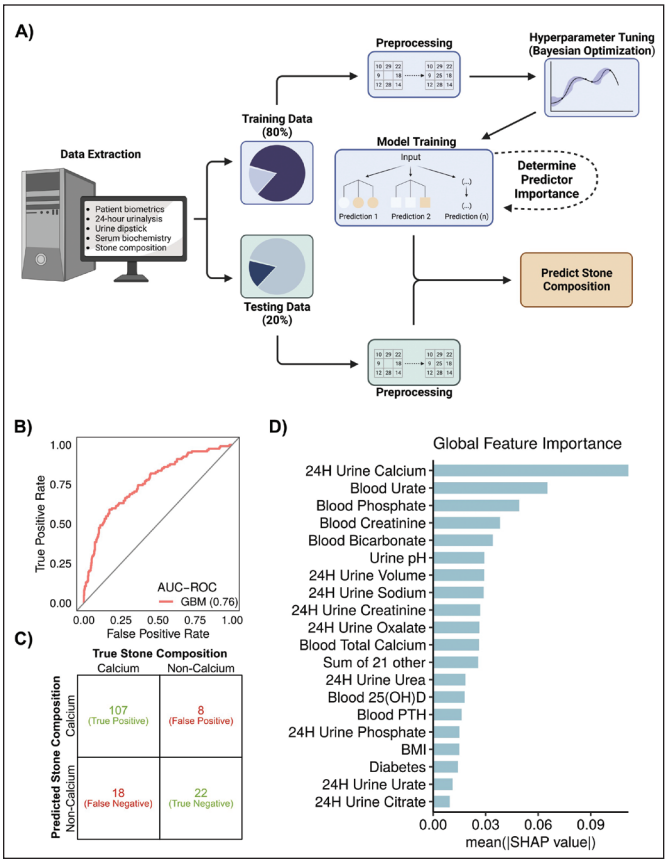

MP 6.17. Figure 1.

Conclusions: This study demonstrates that clinical data can be used to predict stone composition, which may help urologists determine stone type and guide their management plan before stone treatment. Moreover, the model provides a better understanding of key clinical features of stone disease, shedding light on the underlying pathophysiology. By extending machine learning algorithms, it will be possible to determine specific compositions of stones and ultimately improve medical therapy for stone formers.

Acknowledgements: This work has been published in The Journal of Endourology, DOI: https://doi.org/10.1089/end.2023.0446.

MP 6.18

Urothelial cancers in females and males exhibit distinct transcriptomic profiles

Jakub Dobruch[1], Natalia Żeber-Lubecka[2,3], Maria Kulecka[2,3], Michalina Dąbrowska[2], Aneta Bałabas[3], Jerzy Ostrowski[2,3], Konrad Bilski[1]

[1]Department of Urology, Centre of Postgraduate Medical Education, Warsaw, Poland; [2]Department of Gastroenterology, Hepatology and Clinical Oncology, Centre of Postgraduate Medical Education, Warsaw, Poland; [3]Department of Genetics, Maria Skłodowska-Curie National Research Institute of Oncology, Warsaw, Poland

Introduction: Bladder cancer remains 3–4 times more prevalent in men than in women. At the same time, women present with more advanced disease, and despite numerous adjustments, have worse prognoses than their male counterparts. We have previously shown that urobiome diversity is associated with the gender gap. Herein, we evaluated differences of the transcriptomic profiles between bladder cancer (BCa) and healthy bladder mucosa (HBM) found in female and male patients.

Methods: BCa and HBM samples were prospectively collected from 100 female and 100 male patients subjected to primary transurethral resection of bladder tumor (TURBT). Gene expression was analyzed by deep sequencing of tissue's transcriptomes (RNA seq), and differentially expressed genes were identified using the Wald's test.

Results: RNA seq identified 10 402 and 4631 differentially expressed (adjusted p-values ≤0.05) genes, in a pair-wise comparison of BCa vs. HBM, in males and females, respectively. Of these, 3044 and 761 genes were upregulated in BCa samples, in males and females, respectively. Additionally, over three-fold change of expression was observed for 32 genes (top: ITLN1, NNAT, MMP1, CTSE, MUC2, PSORS1C2, TCN1, MUC3A, UGT2B15, IGF2, SPP1) in males, and for 14 genes in females (MMP11, PAX8, HILPDA, RHBG, including seven lncRNA genes). In females, functional enrichment analysis revealed differences related mainly to constitutive signaling by aberrant PI3K in cancer, while in males involved beta-catenin-independent WNT signaling, oxygen-dependent proline hydroxylation of hypoxia-inducible factor alpha and FBXL7 downregulates AURKA during mitotic entry and in early mitosis pathways, among others. In total, we showed 254 and 62 pathways unique to males and females, and 27 common in these comparisons. Combined comparison of males vs. females in BCa and HBM samples revealed that 464 genes were differentially expressed solely in BCa (most significant Reactome pathways: metabolism of steroids; interferon-alpha/beta signaling; class B/2 secretin family receptors) and 96 in HBM samples (only one pathway: HDMs demethylate histones). Depending on the grade of BCa, the analysis showed 1677 (CALML5, ERVH48-1, ANAPC1P6, SPRR1B) and 420 (MUC3A, CTSE, HOXB8) up- and downregulated genes, respectively, in high- compared to low-grade disease.

Conclusions: Female and male bladders affected by urothelial cancers exhibit distinct expression signatures. Molecular alterations observed in males seem to be more complex than in females but both require deeper analysis with numerous covariates taken into consideration.

Acknowledgements: This research was funded by the National Center of Science (Grant NCN nr. 2019/33/B/NZ5/024).